Icarus **143**, 138–146 (2000)
doi:10.1006/icar.1999.6234, available online at http://www.idealibrary.com on IDEAL®

Experiments on Sticking, Restructuring, and Fragmentation of Preplanetary Dust Aggregates

Jürgen Blum and Gerhard Wurm

Astrophysikalisches Institut und Universitäts-Sternwarte, Friedrich-Schiller-Universität Jena, Schillergäßchen 3, D-07745 Jena, Germany
E-mail: wurm@astro.uni-jena.de

Received August 18, 1998; revised March 8, 1999

We performed laboratory as well as microgravity experiments in which we studied the impact of small fractal aggregates consisting of micrometer-sized dust particles onto solid targets at various velocities. Slow bombardment of the target in the laboratory results in the formation of a fluffy dust layer in which gravity-induced compaction is observed. In order to reduce the gravitational aggregate restructuring and, hence, to investigate the collisional behavior of fluffy dust aggregates, we performed additional experiments in the microgravity environment of a drop tower. We observe that the agglomerates are disrupted as long as the impact velocities are above a few meters per second. For slightly lower collision velocities, both sticking to and removal from the target are detected. At even lower velocities, the impinging dust agglomerates are captured by the target with a sticking probability of unity, and a compact dust layer forms. When the impact energies are no longer sufficiently large to allow for agglomerate restructuring, the internal structures of the impacting aggregates are preserved, and we observe the growth of a very porous dust layer. The results of our experiments are in qualitative, but not in quantitative agreement with theoretical predictions. Full quantitative accordance between computer simulations and experiments can be reached when the recently measured values for the rolling friction force $F_{\mathrm{roll}} = 1.2 \times 10^{-9}$ N and for the break-up energy $E_{\mathrm{br}} = 1.3 \times 10^{-15}$ J (valid for 1.9-μm-diameter SiO_2 spheres) are used. Our experimental results suggest that aggregate restructuring in the solar nebula, and hence, the gradual increase of the fractal dimensionality of the dust agglomerates, becomes an important process when the aggregate diameters exceed a few centimeters. Dust aggregates below that size are not expected to be subjected to impact compaction.

Key Words: **solar nebula; planetesimals; experimental techniques; collisional physics; Solar System origin.**

1. INTRODUCTION

The most promising models seeking to explain planetesimal formation are based on a growth mechanism which is due to inelastic collisions between the preplanetary dust grains and adhesive surface forces (Weidenschilling and Cuzzi 1993, and references therein). The mutual collisions are caused by Brownian motion, by differential sedimentation to the nebula's midplane, by radial and transverse drift in the disk, and by turbulence-induced relative velocities. In all these cases, the motion and, therefore, the collisional evolution of the growing aggregates is determined by the interaction of the particles with the nebula gas, as long as the internal gravity of the dust aggregates is negligible, i.e., as long as the sizes of these objects fall below ≈1 km. However, though this general scenario is widely accepted, many details used in the models are still to be considered as *ad hoc* assumptions without experimental verification. In particular, the morphological structures of the evolving dust aggregates and, therefore, their dynamic coupling to the nebular gas motion and their further evolution have hardly been investigated empirically.

The importance of the internal grain structures and the gas–grain dynamics become clear when we consider the growth of an ensemble of dust grains in more detail: Dominated by Brownian motion, the initial collision velocities of the micrometer-sized particles are on the order of 1 mm s^{-1}. As the aggregates grow, i.e., accumulate more mass, velocities due to Brownian motion decrease and the other above-mentioned collision sources become more important. Our earlier experiments have shown that, as long as the collision velocities between the dust aggregates fall below ≈0.2 m s^{-1} and as long as the dust aggregates are small enough (i.e., consist of less than a few hundred micrometer-sized monomers), the dominant growth process is due to sticking collisions between aggregates of very similar sizes (Wurm and Blum 1998). This process produces very fluffy dust agglomerates which can be described using the fractal approach

$$m \propto a_{\mathrm{g}}^{D_{\mathrm{f}}}, \tag{1}$$

in which m, a_{g}, and D_{f} denote the aggregate's mass, its radius of gyration, and the fractal dimension of the growth process. For a growth regime which is dominated by "hit-and-stick" collisions between similar-sized clusters, theoretical (see, e.g., Meakin and Jullien 1988) as well as experimental results (Wurm and Blum 1998) suggest that the value of the fractal dimension is on the order of $D_{\mathrm{f}} \approx 1.9$.

A direct implication of this low fractal dimension $D_{\mathrm{f}} < 2$ is that the gas–grain relaxation time for aggregates

$$\tau_{\mathrm{f}} = \frac{m}{\frac{4}{3}(\delta P)\sigma_{\mathrm{a}}\rho_{\mathrm{g}}v_{\mathrm{m}}} \tag{2}$$

0019-1035/00 $35.00

(Blum *et al.* 1996a) does not increase steeply with growing cluster mass, because the aerodynamic cross section σ_a is almost proportional to the aggregate mass. Here $\delta P = 1.3$, ρ_g, and v_m are the momentum transfer coefficient, the gas density, and the mean thermal velocity of the gas molecules, respectively. A recent work by Kempf *et al.* (1999) showed that for Brownian motion-driven aggregation $\tau_f \propto m^{0.1}$ so that the mean drag force-induced collision velocities in the post-Brownian stage increase at most only by a factor of 5 during the growth of micrometer-sized dust to centimeter-sized fractal aggregates. Therefore, any kind of runaway growth in which a fraction of larger particles moves faster than the remaining bodies and sweeps up all smaller particles is not very likely to start off until a mechanism for the bigger particles to acquire a larger response time to the gas motion (i.e., to become more compact) comes into existence. However, even a slow variation of the response time with mass is mostly offset by the larger collisional cross section of fractal aggregates, so that the temporal evolution of the mean aggregate mass is still efficient (Weidenschilling 1997a).

During this quiescent, non-runaway growth scenario, the initial fractal growth with $D_f < 2$ will continue in quite the same manner until the collisions, at slowly increasing mean velocities but with rising momentum due to the increased projectile masses, are energetic enough for aggregate restructuring to occur. Consequently, the outcoming aggregates of such collisions will be more compact, will have a larger fractal dimension $D_f > 2$, and hence, will possess larger values of τ_f than their precursors. Ultimately, runaway growth will lead to a rapid formation of planetesimals as described in the models by Weidenschilling and Cuzzi (1993) and Weidenschilling (1997b).

However, for a more detailed description and quantitative modeling, the grain restructuring forces and threshold energies for the onset of fractal aggregate compaction need to be determined. Furthermore, knowledge about the threshold energies for total compaction and for aggregate fragmentation is also very desirable for the study of the further evolution of preplanetary dust particles.

Based on a discussion on interparticle forces which act against rolling between contacting spheres of radius a_0, Dominik and Tielens (1995) define a critical torque M_{crit} for the onset of irreversible rolling in aggregate collisions. With this quantity, Dominik and Tielens (1995) introduce the tangential force F_{roll} that can be applied at the center of the particles in order to exceed the yield displacement ξ_{crit} at which rolling starts. Thus, at the onset of irreversible rolling, M_{crit} is balanced by a torque at the contact point, i.e., $M_{crit} = F_{roll} \cdot a_0$. Dominik and Tielens (1995) derived an expression for the absolute value of the rolling friction force in contacts between spherical particles,

$$F_{roll} = 6\pi\gamma\xi_{crit}, \tag{3}$$

in which γ denotes the specific surface adhesion energy. With this model and using the sphere collision model by Chokshi *et al.* (1993), Dominik and Tielens (1997) estimated the outcomes of aggregate–aggregate collisions by computer simulations, and their results suggest to distinguish between the following cases: (1) sticking without restructuring, (2) first visible restructuring, (3) maximum compression, (4) loss of one monomer, and (5) catastrophic disruption. Following Dominik and Tielens (1997), the outcome of an individual collision can be calculated if the impact energy E_{im} (in the center-of-mass frame), the energy for rolling over a quarter of the particle circumference $\pi a_0/2$,

$$E_{roll} = 3\pi^2\gamma a_0\xi_{crit}, \tag{4}$$

the break-up energy

$$E_{br} = 43\frac{\gamma^{5/3}(a_0/2)^{4/3}}{\mathcal{E}^{2/3}}, \tag{5}$$

and the number of contacts in the clusters n_k are known. Here, $\mathcal{E}$ is the reduced modulus of elasticity, given by $1/\mathcal{E} = [(1-\nu_1^2)/\mathcal{E}_1 + (1-\nu_2^2)/\mathcal{E}_2]$, where ν_1, ν_2 and $\mathcal{E}_1$, $\mathcal{E}_2$ mark the Poisson ratios and Young moduli of grains 1 and 2 in contact. Table I summarizes the results from Dominik and Tielens (1997).

TABLE I
The Outcomes of Aggregate Collisions after Dominik and Tielens (1997)

Case	Energy	Collisional outcome
(1)	$E_{im} < 5 \cdot E_{roll}$	Sticking without restructuring
(2)	$E_{im} \approx 5 \cdot E_{roll}$	First visible restructuring
(3)	$E_{im} \approx 1 \cdot n_k \cdot E_{roll}$	Maximum compression
(4)	$E_{im} \approx 3 \cdot n_k \cdot E_{br}$	Loss of one monomer
(5)	$E_{im} > 10 \cdot n_k \cdot E_{br}$	Catastrophic disruption

Note. Here, E_{im}, E_{roll}, E_{br}, and n_k denote the impact energy, the energy for rolling over a quarter of the particle circumference, the break-up energy, and the number of contacts in an aggregate, respectively.

In this article, we present our experiments simulating agglomerate collisions in the solar nebula. We will start with a description of our experimental approach (Section 2); Section 3 summarizes the results from the laboratory experiments (Section 3.1) and from the microgravity experiments (Section 3.2). In Section 4, we compare our experimental results to the model predictions by Dominik and Tielens (1997), and Section 5 presents implications for future modeling of the dust agglomeration in the solar nebula.

2. EXPERIMENTAL APPROACH

Over the past few years, we have developed experimental techniques to study the motion and aggregation of dust particles related to processes in the early Solar System. These studies ranged from the observation of Brownian motion in rarefied gases (Blum *et al.* 1996a) to the analysis of the temporal evolution of fractal aggregates in a self-interacting turbulent dust–gas

cloud (Wurm and Blum 1998). The instrumental developments for these projects provided us with methods to produce a sufficiently large number of fractal aggregates with different sizes and velocities and to use such dust clusters for subsequent experimental studies. On the one hand, this enabled us to observe, for the first time, single aggregate–aggregate collisions due to relative sedimentation (Wurm and Blum 1998); on the other hand, we used the aggregates for cluster–target collisions in which we directed a beam of clusters to a fixed target and observed the outcomes of the impacts at different velocities under normal laboratory conditions as well as in a microgravity environment. This paper will deal with these types of "target experiments."

2.1. *Experimental Setup*

The schematics of our experimental approach are shown in Fig. 1a. A well-characterized particle sample is injected into a turbomolecular pump (TMP) by a small amount of gas (typically 1 cm^3 air at standard pressure). In the TMP, the dust powder is deagglomerated by subsequent collisions with the rotor blades (Blum *et al.* 1996b). Due to the reduction of the outlet of the TMP, the dust grains are efficiently prevented from leaving the turbulent part of the apparatus and, hence, are forced to grow with time to form fractal aggregates with $D_f \approx 1.9$ (for details, refer to Wurm and Blum 1998). Due to the pressure difference between the TMP and the adjacent pre-evacuated experiment chamber, dust aggregates are continuously extracted. As the pressure differential diminishes, the velocity of the gas and, therefore, the extraction velocity of the aggregates decreases with time. Since the outlet of the TMP is shaped as a nozzle, the dust agglomerates enter the experiment chamber in the form of a well-confined jet of less than 1 mm diameter (see Fig. 1b). In the experiment chamber, a tenuous, solid target (thickness 1–10 μm) is mounted at a position intersected by the cluster jet. Outside of the vacuum chamber, a long distance microscope with a working distance of $\approx$80 mm is adjusted to observe the spatial region around the target surface during its collisional interaction with the dust aggregates. The microscope is equipped with a digital CCD camera (256×256 pixels) which acquires full images at 75 Hz frame rate for 12 s. The spatial resolution of the microscopy system is $\approx$1 μm, and the field of view is approximately 0.25×0.25 mm.

We performed two sets of experiments with this setup: (1) In the laboratory, we studied the aggregation of the dust clusters approaching the target at sedimentation velocities which were

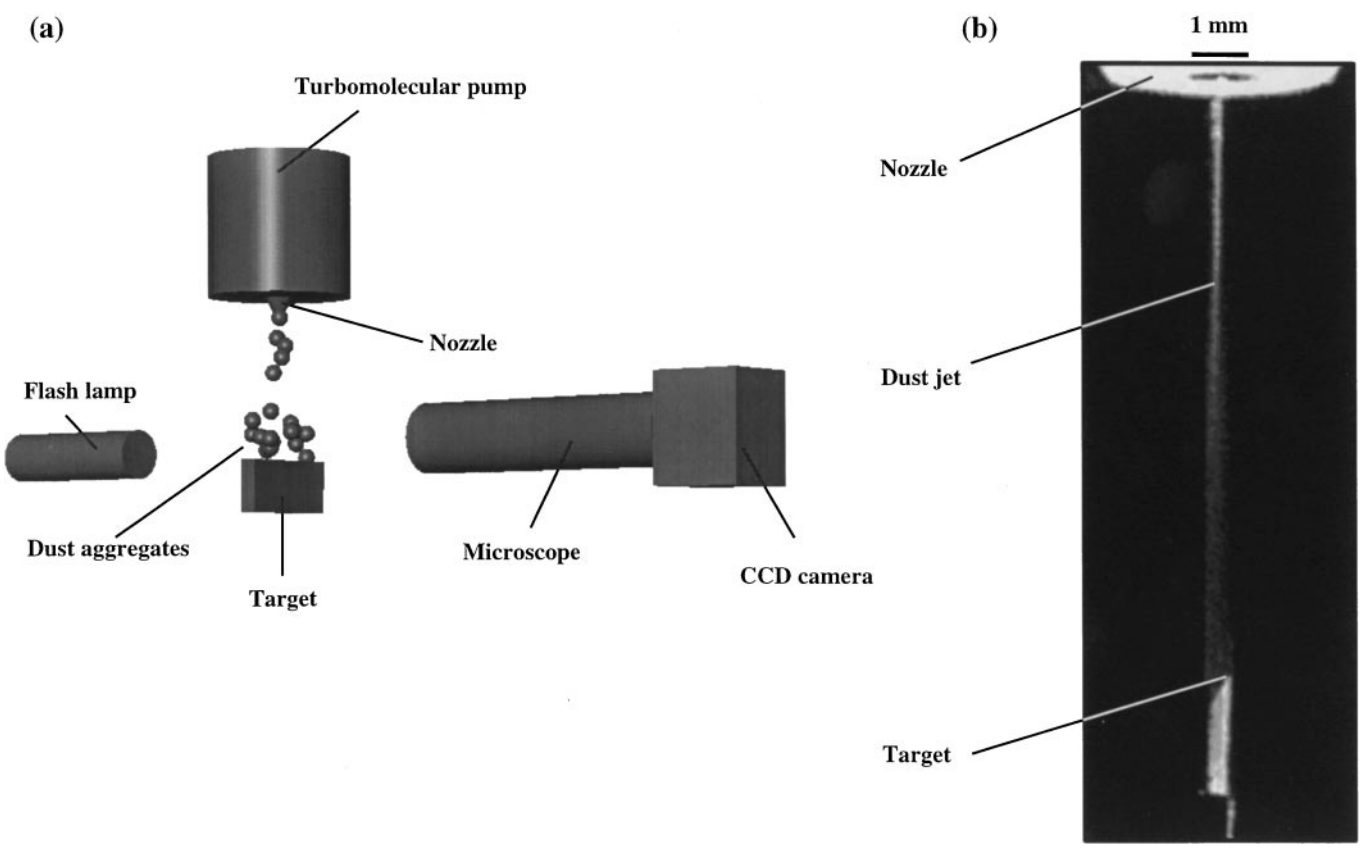

FIG. 1. (a) Sketch of the experimental setup for the laboratory as well as for the drop tower experiments. (b) A video image from the dust jet emerging the nozzle and reaching the target is shown.

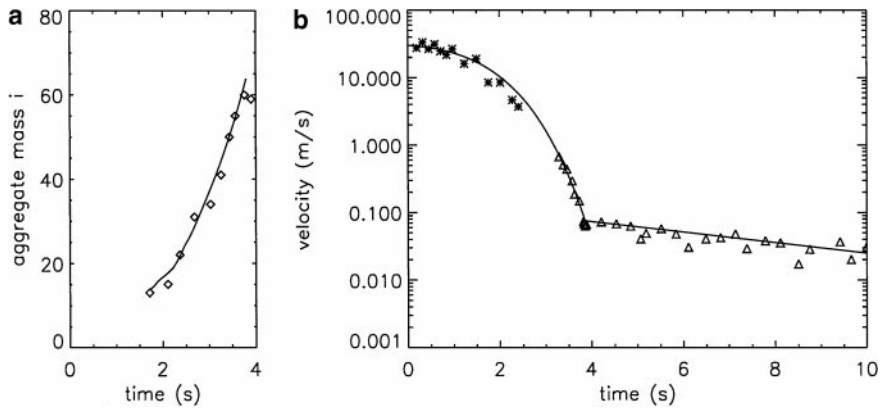

FIG. 2. Agglomerate masses (diamonds) in units of the monomer mass m_0 (a) and impact velocities of these aggregates (b) as functions of the time after injection of the dust sample into the TMP. Velocities were measured by stroboscopic laser (triangles) and flash lamp (asterisk) technique. The solid line in (a) represents the result from the aggregation model by Wurm and Blum (1998), whereas the line in (b) denotes a simple analytic curve fitted to the data. Mind that the laboratory experiments in which the particles sedimented onto the target were performed for $t \geq 4$ s; the microgravity experiments were performed for $t \leq 4$ s.

typically a few centimeters per second in the ambient air environment of 2 mbar pressure. Gas motion is negligible in these experiments, and only the impact momentum and the gravitational pull play a role in the structural evolution of the growing aggregate layer. As it turns out, the effect of gravity is such that these experiments are suitable to estimate the rolling friction force. (2) For a gravitationally undisturbed observation of aggregation processes, we performed a second set of experiments in the drop tower *Bremen*. In these experimental runs, we observed the small fractal agglomerates impacting the target with temporally decreasing velocities, and we recorded the outcomes of these collisions at the maximum temporal and spatial resolution. Typical gas pressures were 2 mbar.

2.2. Dust and Target

The main body of our experiments was performed with a well-characterized sample of dust particles consisting of monodisperse SiO_2 spheres with radius $a_0 = 0.95$ μm and mass $m_0 = 7.2 \times 10^{-15}$ kg. Prior to the experiments, the particles were coated with a silicon-organic mantle (dimethyldimethoxysilane, $(CH_3)_2Si(OCH_3)_2$) to guarantee a nonpolar, hydrophobous surface layer. In the literature, values for the reduced modulus of elasticity for SiO_2 fall within the range $\mathcal{E} = 3.7 \ldots 5.4 \times 10^{10}$ N m^{-2} (Spinner 1962, Shand 1958).[1] Recent measurements of the specific surface energy for micrometer-sized SiO_2 particles yield values between $\gamma = 0.025$ J m^{-2} (Kendall *et al.* 1987) and $\gamma = 0.014 \pm 0.002$ J m^{-2} (Heim *et al.* 1999). In order to determine the specific surface energies of our coated particles, we measured the adhesion force of our SiO_2 spheres relative to the adhesion force of the uncoated particles of Heim *et al.* (1999) using atomic force microscopy. We found that due to the silicon-organic mantle, the specific surface energy of the SiO_2 spheres was increased by a factor of 1.35 ± 0.23. Thus we conclude that our particles have a specific surface energy of $\gamma = 0.019 \pm 0.006$ J m^{-2}.

For these particles, we determined in the laboratory the temporal evolution of the mean number of monomers $i(t)$ in an aggregate as well as of the impact velocity $v(t)$ of the aggregates onto the target (Fig. 2). The aggregate masses increase monotonically with time and reach after 4 s the equivalent of $i = 60$ monomer masses (Fig. 2a). As can be seen in Fig. 2b, the impact velocities decrease very rapidly during the first 4 s, so that the aggregates leave the nozzle at sedimentation velocity for $t > 4$ s. In a microgravity environment, the dust jet characteristics are identical with the exception that the jet of dust particles is terminated at $t \approx 4$ s and no sedimentation phase can be found. Due to the free fall height of the drop tower *Bremen* of 110 m, the microgravity duration is 4.74 s which matches the experiment duration very well.

Besides the dust material mentioned above, we also used monodisperse spheres of $a_0 = 0.5$ μm SiO_2 and irregular grains of $a_0 \leq 1.25$ μm $MgSiO_3$. In the laboratory experiments, targets consisted of a 10-μm-thick steel foil, and in the drop tower experiments, we used ≈ 1 μm thick Si_3N_4 as a target.

3. RESULTS

3.1. Laboratory Experiments

The sedimentation velocity of a beam of dust particles is different from that of a single dust grain (whose gas relaxation time can be calculated using Eq. (2)) due to cumulative effects on the gas motion by the dust aggregates in the jet. Thus, the dust aggregates in the jet hit the target at a speed larger than the free sedimentation velocity $v_s = \tau_f g_0$, in which $g_0 = 9.81$ m s^{-2} is the gravitational acceleration of the Earth. We measured the impact

[1] The mechanical properties were derived for pure silica (SiO_2) glass with a density of 2200 kg m^{-3}. The SiO_2 particles in our sample have a density of 2000 kg m^{-3}. Therefore and due to a lack of better data, we base our further discussion on the lowest literature value for the reduced modulus of elasticity.

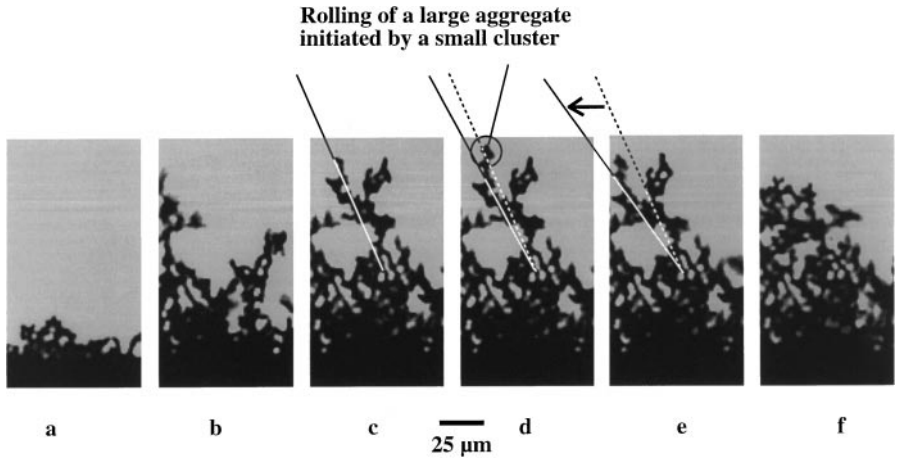

FIG. 3. Sequence of images from the laboratory experiments showing the temporal evolution of the aggregate layer. Due to gravitational restructuring, the porosity of the dust layer decreases with time. (c–e) show a slow restructuring event which was initiated by the addition of an impacting small cluster.

velocity of the jet particles and found that it ranged from $v_s \approx 7\,\mathrm{cm\ s^{-1}}$ to the limiting value of isolated aggregates of $v_s \approx 2.5\,\mathrm{cm\ s^{-1}}$ which was reached after a few seconds (see Fig. 2b). Figure 3 shows a sequence of images from our laboratory experiments. It is clearly visible that a growing layer of dust is forming (Figs. 3a–3f). This already suggests that the sticking probability of the impinging fractal aggregates is unity, and a comparison to the results obtained by Wurm and Blum (1998) verifies this hypothesis. If the incoming aggregates were not subjected to restructuring during the collisions with the growing dust layer, the porosity of the resulting macroscopic aggregate would remain constant. However, as can be seen from the temporal evolution in Fig. 3, the underlying layers of dust get more and more compressed as the thickness of the dust conglomerate is increased. Again, a comparison to our earlier publication (Wurm and Blum 1998) shows that the impact energies are well below the lower limit for impact-driven restructuring. Hence, gravitational restructuring plays the dominant role during the growth of the aggregate layer in our laboratory experiments. We utilize this effect to estimate the resistance force to gravitational restructuring, i.e., the rolling friction force.

In the search for individual agglomeration processes which can be used for the determination of friction forces, we observed several collisions in which the gravitational restructuring is manifested through a slow morphological transition within the aggregate layer (see Figs. 3c–3e). In these cases, the gravitational torque of a single aggregate's lever arm is just overcompensating the resistant torque exerted by the rolling friction force. Hence, we can write to a good approximation for the absolute value of the rolling friction force

$$F_{\mathrm{roll}} = m g_0 \frac{a_{\mathrm{cm}}}{a_0}, \tag{6}$$

where a_{cm} is the horizontal projection of the distance from the center of gravity of the rotating aggregate to the point of contact about which the restructuring occurs. Due to the two-dimensional observation with our long distance microscope, we corrected the visible projected area to the total mass m of the aggregates using the formalism described in Wurm and Blum (1998). Assuming random orientation of the aggregates, we corrected the projected length of the lever arm by a factor of $\sqrt{2}$.

The analysis of several temporally resolved restructuring events yields a mean rolling friction force of $F_{\mathrm{roll}} = (5.0 \pm 2.5) \times 10^{-10}$ N. Mind that aggregates with a gravitational pull exceeding the rolling resistance by a large factor are restructured so quickly that we could not resolve the compaction process, whereas aggregates which were much smaller than the threshold size showed a "hit-and-stick" behavior with no sign of morphological changes.

3.2. *Microgravity Experiments*

To reduce the gravitational compaction of the aggregate growing on the target, we performed the same types of experimental runs in a microgravity environment. Here, we directed the jet of aggregates onto a ≈1-μm-thin surface of an atomic force microscope's cantilever and observed the impact of the aggregates onto this smooth target.

As long as the impact velocities are larger than $1.9 \pm 0.3\,\mathrm{m\ s^{-1}}$, no sticking of the aggregates to the substrate can be observed. On the contrary, we observed that aggregates were disrupted at velocities exceeding a few meters per second. Figure 4 shows examples of fragmentation events in which aggregates hit the surface of the target at $v \geq 5\,\mathrm{m\ s^{-1}}$. The emerging fragments which were recorded within a few microsecond after the impact can easily be distinguished and traced back to a common origin. Due to the tenuousness of the target, the fragments can pass the target on both sides and are, hence, also visible beyond the opposite side of the impact spot.

When, according to Fig. 2, the impact velocities drop below $v = 1.9 \pm 0.3\,\mathrm{m\ s^{-1}}$, the target starts to accumulate single

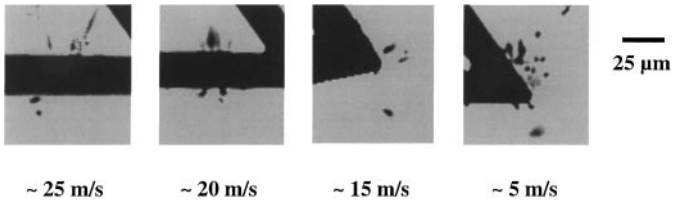

FIG. 4. Images from the drop tower experiments I. Examples from fragmentation events. Aggregates hit the target from below and are disintegrated into their constituents. Due to the tenuousness of the target (target thickness $\approx 1\ \mu$m), the fragments can pass the target on both sides and are, hence, also visible beyond the opposite side of the impact spot. Mind that the emerging fragments leave the field of view within a few microseconds and are, thus, hard to observe. The elongated shapes of the fragments at larger impact velocities are caused by the finite duration of the illumination pulse (1 μs) and make it possible to conclude that different fragments arise from a common impact.

impacting aggregates. However, in the velocity range $1.9 \pm 0.3 \geq v \geq 1.2 \pm 0.2\ \mathrm{m\,s^{-1}}$, both sticking to and removal from the target are in approximate equilibrium (Figs. 5b–5f). At slightly lower impact velocities, i.e., for $v < 1.2 \pm 0.2\ \mathrm{m\ s^{-1}}$, a rapid growth with a sticking probability of unity produces a rather compact agglomerate on the target (Figs. 5g–5p). The open, fractal structures of the impinging agglomerates are totally lost in the collision, and the surface of the growing dust grain assemblage is smooth with irregularities extending only along the impact direction. From this, we conclude that impact compaction is the dominant process in this velocity regime.

In the subsequent transition regime $0.65^{+0.15}_{-0.10} \geq v \geq 0.20^{+0.07}_{-0.05}\ \mathrm{m\,s^{-1}}$, the growth process creates surface irregularities extending also perpendicular to the impact direction. Thus, the impact restructuring cannot be completed before the impact energy is dissipated by friction forces. This phase is succeeded by a structure-preserving growth phase as soon as the impact velocities drop to $v < 0.20^{+0.07}_{-0.05}\ \mathrm{m\,s^{-1}}$. In Fig. 6, we have plotted a few examples of the final growth phase which leads to the formation of a very porous and (due to the absence of gravity) uncompressed dust layer.

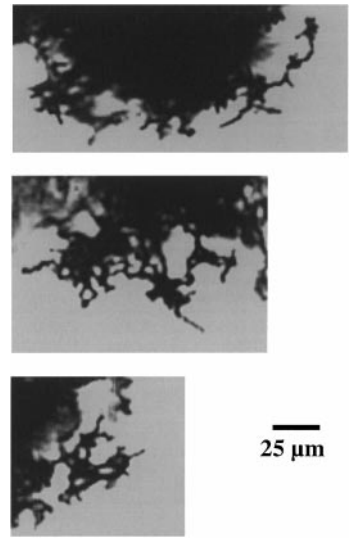

FIG. 6. Images from the drop tower experiments III. Here, the final growth phase in which the agglomerates "hit and stick" to the target with $v < 0.2\ \mathrm{m\,s^{-1}}$, thus forming a porous rim, is shown.

Additional drop tower experiments were performed with two other dust samples. The qualitative behavior of these grains is identical to the processes just mentioned. As we did not measure agglomerate sizes for the other grain types, a quantitative comparison between the three different types of samples is only feasible for the onset of the compact growth phase. In Table II, we have summarized the results of the determination of the critical velocity at which compact agglomeration with a sticking probability of unity starts.

We can see from Table II that agglomerates consisting of smaller grains from the same material have a higher sticking threshold than those consisting of larger monomers. It should be mentioned that a transition regime from perfect sticking to perfect rebound was not detectable for the smaller SiO_2 grains. Aggregates consisting of irregular grains of approximately the

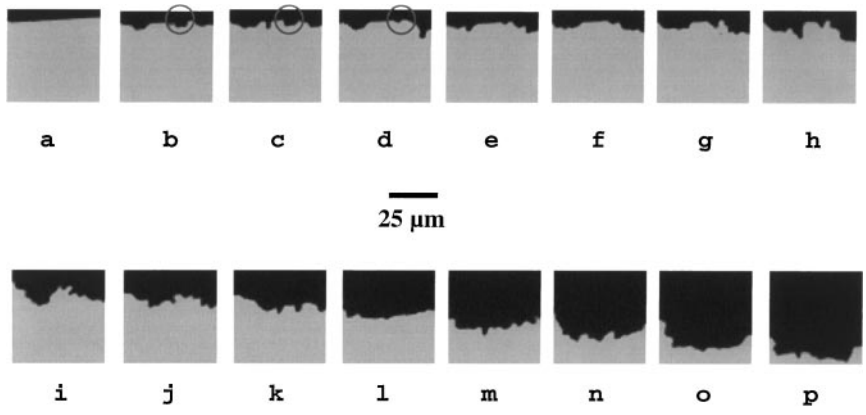

FIG. 5. Images from the drop tower experiments II. Dust agglomerates hit the $\approx$1-μm-thick target (which is shown in (a) before any sticking occurs) from below. (b–p) show a continuous series of images which were taken every 0.013 s. According to Fig. 2, the impact velocities for (b), (g), and (p) are $v = 1.4$, 1.2, and 0.8 m s^{-1}, respectively. For $v \geq 1.2\ \mathrm{m\ s^{-1}}$, sticking and removal of particles are in approximate equilibrium (see circles in (b–d)), and for $v < 1.2\ \mathrm{m\ s^{-1}}$ the rapid formation of a compact dust agglomerate (shown in black) can be observed.

TABLE II
Comparison of the Critical Velocity below which Compact Agglomeration Starts for Three Different Dust Samples

Sample material	Grain size a_0 (μm)	Grain shape	Threshold velocity (m s^{-1})
SiO_2 (coated)	0.95	Spherical	1.2 ± 0.2
SiO_2 (uncoated)	0.50	Spherical	3.1 . . . 3.9
$MgSiO_3$	<1.25	Irregular	1.6 . . . 2.8

same size as the larger SiO_2 particles show also an increased threshold velocity for sticking. A very similar sticking behavior was found by Poppe *et al.* (1999a). In this publication, the authors state that the capture limit for single micrometer-sized spherical particles is increasing with decreasing grain size and that irregular-shaped dust grains in general have a higher capture velocity than spherical grains of the same size.

4. DISCUSSION

In contrast to the laboratory experiments, which were carried out for $t > 4$ s, the aerodynamic drag forces of the rarefied gas stream on the aggregates sticking to the target are no longer *a priori* negligible in the microgravity experiments, and the relative importance of the dust impacts and gas drag must be estimated. For that, we have measured the local dust particle number density in the jet. It turns out that the local mass density of the solid particles in the jet exceeds the gas density by a factor of $\approx$100. The local gas velocity in the jet region is equivalent to the dust particle velocity, as the friction time scale τ_f is a few milliseconds, so that the dust particles couple perfectly to the gas motion within a few millimeter after leaving the nozzle. To check the momentum transfer due to the dust impacts, we have measured the average force exerted by the ensemble of dust particles in the jet on an atomic force microscope cantilever. It turns out that the maximum total impact force is $\approx 10^{-5}$ N. The maximum impact velocity of the dust grains onto the cantilever is 30 m s^{-1} (see Fig. 2), requiring a particle flux onto the cantilever's surface of $\approx 5 \times 10^7$ s^{-1}, which is in good agreement to our measurements. With the Epstein gas drag formula,

$$F_{\rm drag} = \frac{4}{3}\sigma_{\rm a} v \rho_{\rm g} v_{\rm m}, \tag{7}$$

in which σ_a, ρ_g, and v_m are the aerodynamic cross section of the cantilever, the gas density, and the mean thermal velocity of the gas molecules, respectively, we can calculate the net force of the streaming gas. For $\sigma_a = 1 \times 10^{-9}$ m^2 (i.e., the area of the cantilever impacted by dust particles), $\rho_g = 2.6 \times 10^{-3}$ kg m^{-3}, $v = 30$ m s^{-1}, and $v_m = 475$ m s^{-1}, we get $F_{\rm drag} = 5 \times 10^{-8}$ N, more than two orders of magnitude smaller than the impact force exerted by the dust grains. This means that the average momentum transfer by the gas stream is negligible with respect to the impulse of the impacting particles.

A recent direct measurement of the rolling friction force by Heim *et al.* (1999) using modified atomic force microscopy yields for uncoated 1.9-μm SiO_2 spheres a value of $F_{\rm roll} = (8.5 \pm 1.6) \times 10^{-10}$ N, in contrast to the estimates given by Dominik and Tielens (1995) who calculated $F_{\rm roll} = 4.7 \times 10^{-11}$ N. Obviously, the measured data exceed the predicted value by more than one order of magnitude, but one should mind, however, that the value for the critical displacement before irreversible restructuring occurs, $\xi_{\rm crit} = 10^{-10}$ m (see Eq. (3)), was just a model assumption and probably underestimated by Dominik and Tielens (1995) (a more detailed discussion on this topic can be found in Heim *et al.* (1999)). For comparison of the results of our impact experiments with the simulations by Dominik and Tielens (1997), we correct the rolling friction force as determined by Heim *et al.* (1999) to account for the silicon-organic mantle. Using the proportionality between $F_{\rm roll}$ and γ (Eq. (3)) and a ratio between the specific surface energies of coated and uncoated spheres of 1.35 ± 0.23 (Section 2.2), we derive $F_{\rm roll} = (11.5 \pm 4.1) \times 10^{-10}$ N. This value corresponds to our coarse estimate of $F_{\rm roll} = (5.0 \pm 2.5) \times 10^{-10}$ N within one standard deviation. In the following discussion we will use $F_{\rm roll} = (11.5 \pm 4.1) \times 10^{-10}$ N due to the higher reliability of the measurements by Heim *et al.* (1999).

With the revised value for the rolling friction force, we can, according to Table I, calculate the threshold velocities for the onset of restructuring and for total compaction in aggregate–aggregate collisions. Following Dominik and Tielens (1997), the onset of restructuring occurs when the impact energy reaches the critical value $E_{\rm im} = 5E_{\rm roll} \approx (5/2)F_{\rm roll}\pi a_0$. As the transition between morphology-conserving impacts and restructuring occurred toward the lower end of our investigated velocity regime, the corresponding mean aggregate mass in our experiments was $m \approx 60\ m_0$ (see Fig. 2). Thus, the critical velocity above which grain restructuring occurs is $v_{\rm restr,theo} = \sqrt{10E_{\rm roll}/m} = 0.20 \pm 0.04$ m s^{-1}. This is in excellent agreement with our measured value $v_{\rm restr,meas} = 0.20^{+0.07}_{-0.05}$ m s^{-1} (see Section 3.2).

The velocity range in which sticking with complete compression dominates should, thus, start at $v_{\rm compr} = \sqrt{2E_{\rm roll}/m_0} = 0.69 \pm 0.12$ m s^{-1}, when we assume that the number of contacts in an aggregate, is given by

$$n_{\rm k} \approx m/m_0, \tag{8}$$

which is justified by the low fractal dimension $D_f \approx 1.9$ of the clusters in the dust jet (see Wurm and Blum (1998)). This value for $v_{\rm compr}$ is also in very good agreement with our observations that maximum compaction occurs for $v > 0.65^{+0.15}_{-0.10}$ m s^{-1}. Thus, we conclude that for the friction force-dominated aggregate collision regime, the results from simulations by Dominik and Tielens (1997) are in excellent accordance with those from our experiments as long as the revised rolling friction forces from Heim *et al.* (1999) are applied to the model.

In addition to the velocity regime for restructuring, Dominik and Tielens (1997) estimated the energy range in which the transition from sticking (with full compaction) to rebound (with

TABLE III
Comparison between Experimental and Model Values for the Threshold Velocities of the Collisional Outcome Cases from Table I

Case	Energy	Experimental velocity (m s^{-1})	Model velocity (m s^{-1}) with new data for E_{roll} and E_{br}[a]	Model velocity (m s^{-1}) with old data for E_{roll} and E_{br}[b]
(2)	$E_{im} \approx 5 \cdot E_{roll}$	$0.20^{+0.07}_{-0.05}$[c]	0.20 ± 0.04[c]	0.047[c]
(3)	$E_{im} \approx 1 \cdot n_k \cdot E_{roll}$	$0.65^{+0.15}_{-0.10}$	0.69 ± 0.12	0.16
(4)	$E_{im} \approx 3 \cdot n_k \cdot E_{br}$	1.2 ± 0.2	1.0	0.14
(5)	$E_{im} > 10 \cdot n_k \cdot E_{br}$	1.9 ± 0.3	1.9	0.26

[a] $E_{roll} = 1.7 \times 10^{-15}$ J from Heim *et al.* (1999). $E_{br} = 1.3 \times 10^{-15}$ J from Poppe *et al.* (1999a,b).
[b] $E_{roll} = 9.5 \times 10^{-17}$ J from Dominik and Tielens (1995). $E_{br} = 2.4 \times 10^{-17}$ J from Chokshi *et al.* (1993) and Dominik and Tielens (1997).
[c] Valid for $m = 60 m_0$.

complete fragmentation) occurs to

$$E_{st} = (3 \ldots 10) n_k E_{br} \tag{9}$$

(see Table I). Using again the fractal nature of the particles (Eq. (8)) and the expression for the break-up energy of a single contact given by Dominik and Tielens (1997) (Eq. (5)), $E_{br} = 2.4 \times 10^{-17}$ J, one obtains for the velocity threshold for sticking $v_{st} = \sqrt{2(3 \ldots 10) E_{br}/m_0} = 0.14 \ldots 0.26$ m s^{-1}. This is clearly in contradiction to our results from Section 3.2 where we describe that the transition from rebound to sticking occurs at $v_{st} = 1.2 \pm 0.2 \ldots 1.9 \pm 0.3$ m s^{-1} and to the earlier results by Wurm and Blum (1998) that sticking without restructuring is the dominant process for fractal aggregates which collide with $v \leq 0.2$ m s^{-1}.

Experiments by Poppe *et al.* (1999a) show that single spherical SiO_2 grains colliding with a flat SiO_2 target have a capture threshold of

$$v_{st} \approx 0.92 \left(\frac{a_0}{\mu \mathrm{m}} \right)^{-0.52} \mathrm{m\ s^{-1}}, \tag{10}$$

obviously at much higher velocities than calculated by Chokshi *et al.* (1993) and Dominik and Tielens (1997). Within the experimental uncertainties, these results are also valid for SiO_2 spheres coated with silicon-organic mantles (Poppe *et al.* 1999b). If we use the argument put forward by Dominik and Tielens (1997) that the break-up process will use up the same energy as is dissipated during a collision with the capture threshold velocity, we can derive from Eq. (10) an empirical value for the break-up energy of the 1.9-μm SiO_2 spheres in our experiments:

$$E_{br} = \frac{1}{2} \left(\frac{1}{2} \right)^{4/3} m_0 v_{st}^2 = 1.3 \times 10^{-15} \text{ J}. \tag{11}$$

The correction factor $(\frac{1}{2})^{\frac{4}{3}}$ in the center part of Eq. (11) reflects the scaling from a particle–wall interaction to a particle–particle contact. Inserting this result into Eq. (9), we get for the capture threshold $v_{st,theo} = \sqrt{2E_{st}/m} = 1.0 \ldots 1.9$ m s^{-1} which is in excellent agreement with our observed velocity regime $v_{st,meas} = 1.2 \pm 0.2 \ldots 1.9 \pm 0.3$ m s^{-1}. In particular, the lower limit of this velocity range corresponds very well to our detection that the growth phase reaches at $v = 1.2 \pm 0.2$ m s^{-1} a sticking probability of unity.

From the previous paragraphs, we conclude that the model simulations by Dominik and Tielens (1997) describe the measured process sequence very well, i.e., in decreasing velocity order: fragmentation, sticking with partial mass loss, sticking with maximum compaction, and unrestructured sticking. The actual predicted velocities, however, are underestimated by up to one order of magnitude and are in obvious disagreement with the experimental findings of this paper as well as of earlier work on coagulation and aggregation (Wurm and Blum 1998, Poppe *et al.* 1999a,b). Inserting new experimental values for the rolling friction force and for the break-up energy yields an almost perfect match between the predictions by the simulations of Dominik and Tielens (1997) and the experimental results presented in this paper. For a better comparison, we have summarized these results in Table III.

5. APPLICATIONS TO THE PREPLANETARY DUST AGGLOMERATION

With the above-mentioned results from our experiments and the excellent agreement between these measurements and the simulations by Dominik and Tielens (1997) using the revised data for the friction force and the break-up energy (see Table III), we are able to describe the physical behavior of preplanetary dust agglomerates and their collisional growth. These data are important for the modeling of the growth time scales of preplanetary bodies. In his latest model, Weidenschilling (1997a) uses (among others) an initial fractal dimension of $D_f = 1.95$ for the preplanetary dust aggregates, which is, according to Wurm and Blum (1998), the most realistic value. Due to sedimentation of the grains to the nebula's mid-plane, the overall mass density of the solids increases steadily with time. Weidenschilling (1997a) stopped his simulation when settling

had produced a particle layer with a spatial density in the central plane of $3M_\odot/2\pi r^3$, equivalent to the classical value for gravitational instability. Here, $M_\odot$ and r are the solar mass and the distance from the Sun, respectively. At $r = 1$ AU, this criterion is equivalent to a solids/gas mass ratio of 76 (Weidenschilling 1997a). To account for impact restructuring, Weidenschilling (1997a) assumed a size limit $a_{\rm cr}$ above which the mass density of the aggregates remains constant (and, hence, the fractal dimension is increased to $D_{\rm f} = 3$). In his model, Weidenschilling (1997a) assumed values $a_{\rm cr} = 0.1 \ldots 10$ mm.

Based on the results of the previous sections, we will estimate the critical size for an aggregate above which it is restructured in mutual collisions. We use again the model by Dominik and Tielens (1997), which is in accordance with our experimental results (Section 4), but using the new values for the rolling friction force (of uncoated particles) of SiO_2, $F_{\rm roll} = 8.5 \times 10^{-10}$ N (Heim *et al.* 1999). If we assume a mean collision velocity of the agglomerates in the post-Brownian growth regime of $v = 0.1$ mm s^{-1}, we can calculate the minimum mass and size of the fractal agglomerates before restructuring occurs. After Table I,

$$\tfrac{1}{2}\mu v^2 > \tfrac{5}{2}\pi a_0 F_{\rm roll}, \tag{12}$$

where μ is the reduced mass of the two colliding aggregates which we assume to be of equal size. Taking $a_0 = 1$ μm and $m_0 = 8.4 \times 10^{-15}$ kg, we get for the critical mass $m_{\rm cr} \approx 2.7 \times 10^{-6}$ kg. This mass corresponds to a critical aggregate radius of $a_{\rm cr} = 32$ mm, when we follow the mass-size relation given by Mukai *et al.* (1992),

$$\frac{m}{m_0} = 0.53\left(\frac{a}{a_0}\right)^{D_{\rm f}}, \tag{13}$$

with $D_{\rm f} = 1.95$.

It should be noted that this critical size above which restructuring occurs is larger than the maximum $a_{\rm cr}$ assumed by Weidenschilling (1997a). However, the choice of $a_0 = 1$ μm is rather arbitrary and might not exactly fit the solar nebula conditions, so that a discussion of the monomer size dependence of $a_{\rm cr}$ is mandatory. If we assume $F_{\rm roll} \propto a_0^\delta$ with the extreme cases $\delta = 0$ (as assumed by Dominik and Tielens (1995)) and $\delta = \frac{2}{3}$ (the size dependence of the contact radius of two spheres as derived by Johnson *et al.* (1971)), and $v \propto \tau_f \propto a_0$ (implying $D_{\rm f} < 2$), we can use Eqs. (12) and (13) to formulate the monomer size dependence of $a_{\rm cr}$

$$a_{\rm cr} \propto a_0^{\frac{D_{\rm f}+\delta-4}{D_{\rm f}}}. \tag{14}$$

With $D_{\rm f} \approx 2$, we get $a_{\rm cr} \propto a_0^{-1}$ for $\delta = 0$ and $a_{\rm cr} \propto a_0^{-2/3}$ for $\delta = \frac{2}{3}$. This means that for smaller initial particle sizes the restructuring threshold size even increases. As Poppe *et al.* (1999b) show, the threshold velocity for sticking of irregular particles exceeds that of spherical grains of the same size so that our new derived values for $a_{\rm cr}$ are possibly lower limits to the maximum fractal aggregate sizes. Therefore, new calculations of the drag-induced growth phase are required, taking into account that fractal growth dominates to sizes of at least several centimeters before impact compaction occurs.

ACKNOWLEDGMENTS

The authors thank O. Minster and the European Space Agency for funding the drop tower experiments and the staff at the Bremen drop tower facility for their hospitality. We thank L.-O. Heim for the determination of the contact forces of coated SiO_2 microspheres. The laboratory experiments were funded by the German Space Agency (DLR) as part of the CODAG program. J.B. and G.W. are supported by DLR Grant 50 QV 9603 0.

REFERENCES

Blum, J., M. Schnaiter, G. Wurm, and M. Rott 1996b. The de-agglomeration and dispersion of small dust particles—Principles and applications. *Rev. Sci. Instrum.* **67**, 589–595 .

Blum, J., G. Wurm, S. Kempf, and Th. Henning 1996a. The Brownian motion of dust particles in the solar nebula—An experimental approach to the problem of pre-planetary dust aggregation. *Icarus* **124**, 441–451.

Chokshi, A., A. G. G. M. Tielens, and D. Hollenbach 1993. Dust coagulation. *Astrophys J.* **407**, 806–819.

Dominik, C., and A. G. G. M. Tielens 1995. Resistance to rolling in the adhesive contact of two spheres. *Phil. Mag. A* **72**, 783–803.

Dominik, C., and A. G. G. M. Tielens 1997. The physics of dust coagulation and the structure of dust aggregates in space. *Astrophys. J.* **480**, 647–673.

Heim, L.-O., J. Blum, M. Preuss, and H.-J. Butt 1999. Adhesion and friction forces between spherical micrometer-sized particles. *Phys. Rev. Lett.* **83**, 3328–3331.

Johnson, K. L., K. Kendall, and A. D. Roberts 1971. Surface energy and the contact of elastic solids. *Proc. Roy. Soc. London A* **324**, 301–313.

Kempf, S., S. Pfalzner, and Th. Henning 1999. *N*-particle simulations of dust growth: I. Growth driven by Brownian motion. *Icarus*, in press.

Kendall, K., N. M. Alford, and J. D. Birchall 1987. A new method for measuring the surface energy of solids. *Nature* **325**, 794–796.

Meakin, P., and R. Jullien 1988. The effects of restructuring on the geometry of clusters formed by diffusion-limited, ballistic and reaction-limited cluster-cluster aggregation. *J. Chem. Phys.* **89**, 246–250.

Mukai, T., H. Ishimoto, T. Kozasa, J. Blum, and J. M. Greenberg 1992. Radiation pressure forces of fluffy porous grains. *Astron. Astrophys.* **262**, 315–320.

Poppe, T., J. Blum, and Th. Henning 1999a. New experiments on collisions of solid grains related to the preplanetary dust aggregation. *Adv. Space Res.* **23**, 1197–1200.

Poppe, T., J. Blum, and Th. Henning 1999b. Analogous experiments on the stickiness of micron-sized preplanetary dust. *Astrophys. J.*, submitted.

Shand, E. B. 1958. *Glass Engineering Handbook*. McGraw–Hill, New York.

Spinner, S. 1962. Temperature dependence of elastic constants of vitreaous silica. *J. Am. Ceram. Soc.* **45**, 394–397.

Weidenschilling, S. J. 1997a. When the dust settles: Fractal aggregates and planetesimal formation. *Proc. Lunar Planet. Sci. Conf. 28th*, 1517–1518.

Weidenschilling, S. J. 1997b. The origin of comets in the solar nebula: A unified model. *Icarus* **127**, 290–306.

Weidenschilling, S. J., and J. N. Cuzzi 1993. Formation of planetesimals in the solar nebula. In *Protostars and Planets III* (E. H. Levy and J. I. Lunine, Eds.), pp. 1031–1060. Univ. of Arizona Press, Tucson.

Wurm, G., and J. Blum 1998. Experiments on preplanetary dust aggregation. *Icarus* **132**, 125–136.